

Polymer Blends with Modified Coupling Agent. I. Preparation and Thermal Properties of LICA 44 Grafted Styrene–Maleic Anhydride Copolymer

WEN-YEN CHIANG, CHIA-HAO HU

Department of Chemical Engineering, Tatung Institute of Technology, 40, Chungshan N. Rd., 3rd Sec., Taipei 104, Taiwan, Republic of China

Received 5 April 1997; accepted 4 September 1997

ABSTRACT: Neopentyl(diallyl)oxy, tri(*N*-ethyleneamino)ethyl titanate (LICA 44) was grafted to the styrene/maleic anhydride (SMA) copolymer for the purpose of obtaining a new interfacial coupling agent for flame retardant ABS blends. The graft reaction was proceeded in DMSO under 80°C and reduced pressure. Samples were prepared under various amine/anhydride ratios (AAR) in feed and reaction time. The verification of reaction was based on FTIR spectra and the results of elemental analysis. The reaction percentages were high but decreased with the rising AAR. Both combination types, amide acid and imide, of SMA and LICA 44 were found, and the ratio of amide acid and imide is related to the AAR and reaction time. After the graft reaction, both the initial pyrolysis temperature (T_{pi}) and the char yield at 800°C of SMA increased significantly. LICA 44 is believed to cause the char promoting effect on SMA-*g*-L44. And the dealcohol phenomenon of trimethylolpropane diallyl ether (TMPDE) away from SMA-*g*-L44 was observed during the thermal analysis. © 1998 John Wiley & Sons, Inc. *J Appl Polym Sci* 68: 37–44, 1998

Key words: SMA; LICA 44; grafting; thermal resistance; char yield

INTRODUCTION

The styrene–maleic anhydride (SMA) copolymer is polymerized from monomers of an extreme polarity difference, and is one of the most investigated copolymer systems. Although SMA is usually an example of typically alternating copolymerization by reason of the strong alternating tendency, Lin et al. reported that the reactivity ratios, r_1 and r_2 , can be changed under some reaction temperatures and solvents employed to get a random copolymer.¹ The mole ratio of styrene in

the copolymer was >0.5 by using the solvent of decalin.

In the field of polymer blends, the SMA copolymer is commonly employed as a reactive compatibilizer in two ways to improve the mechanical properties of polymer blends.^{2–4} One is to couple SMA with a reactive polymer matrix, and the other is to react SMA with a reactive coupling agent. An example of the former case is the coupling of cellulose acetate and SMA.^{5,6} The latter method is usually adopted when the polymer matrices do not have reactive groups, and an example is the approach adopted by C. Koning and his coworkers, who selected an α -amino-polystyrene as a reactive coupling agent to graft on SMA to compatibilize the SMA and poly(phenylene oxide).⁷ The amine groups react with maleic anhydride to form an imide combi-

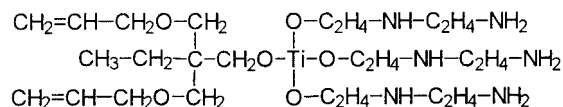
Correspondence to: W.-Y. Chiang.

Contract grant sponsor National Science Council; contract grant number: NSC 86-2216-E-036-001.

Journal of Applied Polymer Science, Vol. 68, 37–44 (1998)

© 1998 John Wiley & Sons, Inc.

CCC 0021-8995/98/010037-08



Scheme 1

nation, and the chemical modified SMA will accumulate and exhibit a compatibilizing effect between two phases in the procedure of blending.⁸ However, the flame-retarded ABS blend is a different system from the above polymer blends, which consists of the matrix and additives, including the flame retardant and the flame-retardant assistant. Besides the organic/organic interface, the organic/inorganic interface also exists in this system. The available approaches for organic/inorganic interface modification include matrix grafting and surface treatment of additives.^{9–14}

The coupling agents of LICA series, produced by Kenrich Petrochemical Inc., are designed for the organic/inorganic interfacial adhesion of polymer composites. Ghosh and Maiti employed LICA 38 to modify the interface of silver powder-filled polypropylene and obtained improved mechanical properties.¹⁵ We also used LICA 44 in the surface treatment of carbon fiber in high-impact polystyrene (HIPS) composites with electromagnetic shielding function.¹⁶ The improved carbon fiber dispersion and wetting on the fiber/resin interface in the HIPS composites is mainly caused by LICA 44. The previous at-

tempts on employing LICA 44 for the surface modification were usually proceeded by solvent-coating or *in situ* reaction in an extruder, but never made by a graft reaction. In this article, we prepared SMA-*g*-L44 in a reactor. The influences of amine/anhydride ratio (AAR) in feed and reaction time on the products were investigated and discussed by means of FTIR, elemental analysis, and thermal analysis.

EXPERIMENTAL

Materials

The styrene/maleic anhydride copolymer (SMA) with a styrene ratio of 66% was provided by Sigma Chemical Co. The average MW of the SMA was estimated about 3718 by the following Houwink–Mark equation:

$$[\eta] = KM^a$$

via a measurement of intrinsic viscosity. The constant K and parameter a of SMA were reported to be 5.046×10^{-5} and 0.9005, respectively in our former article.¹⁷ Neopentyl(diallyl)oxy, tri(*N*-ethyleneamino)ethyl titanate, designated as LICA 44, MW = 570.36, was purchased from Kenrich Petrochemical Inc. The molecular structure of LICA 44 is shown in Scheme 1. Solvents

Table I The Compositions of Reactants in Feed and Reaction Conditions

Sample Code	SMA (mmol)	LICA 44 (mmol)	LICA 44/SMA ^a by mol	AAR ^b by mol	Reaction Temp. (°C)	Reaction Time (h)
A ^c	—	—	0	0	—	—
B	2.42	3.23	1.33	0.5	60	6.0
C	2.69	5.38	2.0	0.8	60	6.0
D	2.42	6.14	2.54	1.0	60	6.0
E	2.69	10.76	4.0	1.5	60	6.0
E05	2.69	10.76	4.0	1.5	60	0.5
E10	2.69	10.76	4.0	1.5	60	1.0
E30	2.69	10.76	4.0	1.5	60	3.0
F	2.42	12.10	5.0	1.9	60	6.0
G	2.69	21.51	8.0	3.0	60	6.0
H	2.69	32.27	12.0	4.5	60	6.0

$$^a \text{LICA44/SMA} = \frac{W_L/M_L}{W_S/M_S}$$

$$^b \text{AAR} = \frac{E_L \times (W_L/M_L)}{E_S \times (W_S/M_S)}$$

^c SMA copolymer, the raw material.

Table II The Estimated and Analyzed Elemental Compositions of Products

Sample Code	Estimated Composition ^a						Reaction Percentage of LICA 44 ^c (%)
	C (wt %)	H (wt %)	N (wt %)	O (wt %)	Ti (wt %)	N ^b (wt %)	
A	78.36	5.98	0	15.67	0	0	0
B	73.59	6.59	2.52	15.86	1.44	2.44	96.8
C	71.76	6.82	3.49	15.94	1.99	3.20	91.7
D	70.48	6.99	4.16	15.99	2.37	3.84	92.3
E	67.69	7.34	5.64	16.11	3.22	4.96	87.9
F	66.18	7.54	6.43	16.17	3.67	5.64	87.7
G	62.92	7.95	8.16	16.30	4.65	5.34	65.4
H	60.23	8.30	9.58	16.42	5.46	5.72	59.7

^a Calculated from the chemical formula of reactants.

^b The weight percent of N in the final product measured by elemental analysis.

^c Obtained by dividing the percent N from elemental analysis with estimated percent N.

large amount of isopropanol for 24 h. The detailed procedure of purification was summarized in Scheme 2, in which sample B was taken as an example.

Characterization of SMA-g-L44

There are two possible combination types for SMA and LICA 44, as shown in Scheme 3. Infrared spectra were obtained in the region of 4000–400 cm^{-1} using a Jasco FTIR E-300 spectrometer to distinguish the amide acid from the imide. The elemental compositions of C, H, and N were measured with a Perkin–Elmer 2400 elemental ana-

lyzer with an accuracy of 0.3% to estimate the product ratios.

Thermal Analysis of SMA-g-L44

The thermal analysis of products was carried out using a DuPont thermal gravimetric analyzer (TGA) model 951, and a differential scanning calorimeter (DSC) model 910. In a typical TGA analysis, the specimen was thermally equilibrated at 60°C and kept isothermally for 5 min to remove the absorbed water, and then heated to 900°C at

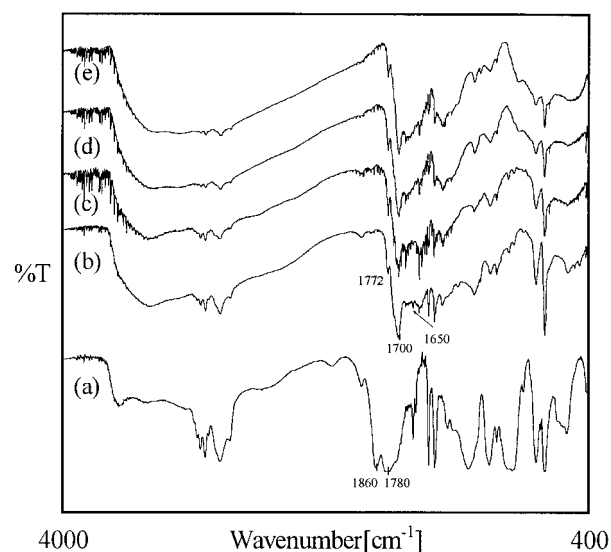


Figure 2 The FTIR spectra of (a) sample A; (b) sample C; (c) sample E; (d) sample G; and (e) sample H.

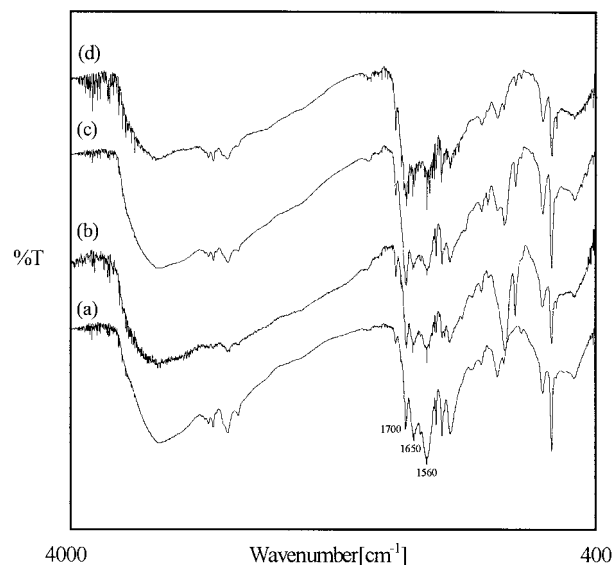


Figure 3 The FTIR spectra of sample E with different reaction time: (a) 0.5 h; (b) 1.0 h; (c) 3.0 h; and (d) 6.0 h.

Table III The Relative Peak Strength of Imide (1700 cm⁻¹) by Peak Integral Analysis

Sample Code	Peak A Area (1700 cm ⁻¹)	Peak B Area (700 cm ⁻¹)	Relative Strength A/B
C	22.72	11.60	1.959
E	4.30	1.78	2.415
E05	6.05	9.11	0.664
E10	10.43	10.87	0.960
E30	16.00	10.08	1.587
G	10.67	3.09	3.453
H	11.80	2.93	4.027

Integrated by the JascoFT analysis software with two-base method.

a heating rate of 20°C/min using a nitrogen flow rate of 40 mL/min. The DSC was proceeded under a heating rate of 10°C/min and a nitrogen flow rate of 30 mL/min. The data analysis of all TGA and DSC thermograms were carried out by using the DuPont TA2000 GENERAL ANALYSIS v4.0 software.

Definition of Amine/Anhydride Ratio (AAR)

The amine/anhydride ratio (AAR) in feed is defined as the following equation:

$$\text{AAR} = \frac{E_L \times (W_L/M_L)}{E_S \times (W_S/M_S)}$$

where W_L and W_S are the weights of LICA 44

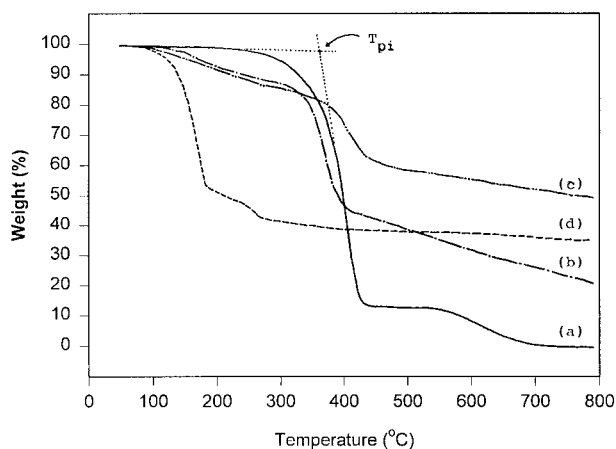


Figure 4 The TGA diagrams of (a) sample A (—); (b) sample E (---); (c) sample H (- · - · -); and (d) LICA 44 (····).

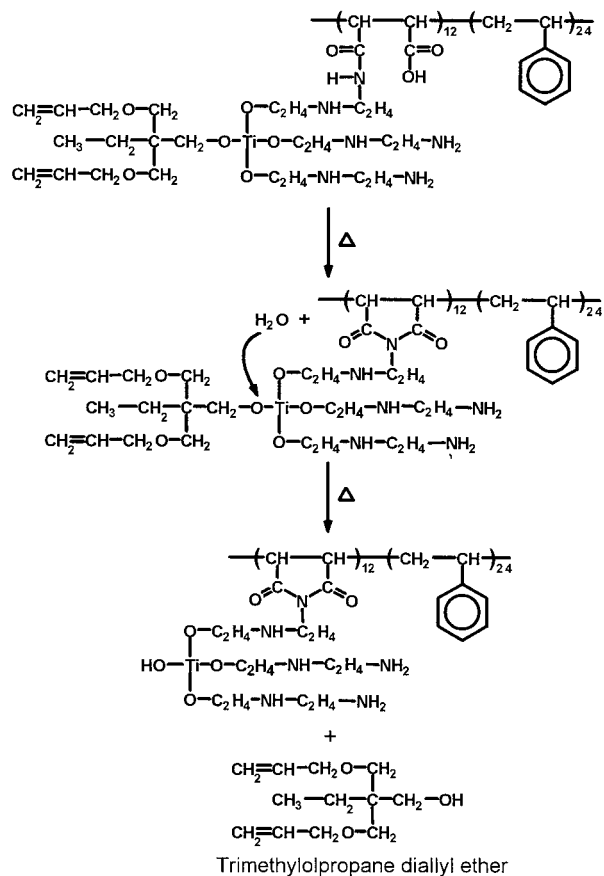


Figure 5 The incidental reaction of SMA-g-L44 under heating.

and SMA in feed; M_L and M_S are the molecular weights of LICA 44 and SMA. There are three primary and three secondary amine in a LICA 44 molecule, and 12 anhydride in a SMA molecule. Hence, the chemical equivalents of LICA 44 and SMA, E and IE_S , should be equal to 9 and 24, respectively.

RESULTS AND DISCUSSION

The Preparation of SMA-g-L44

Both the SMA and LICA 44 were well dissolved in DMSO at the beginning of the reaction, but they became a suspended solution at the end of reaction. The product mixture consisted of SMA-g-L44, unreacted LICA 44, and solvent. The SMA-g-L44 can be separated by the addition of methanol and isopropanol (Scheme 2). The secondary amine in LICA 44 is considered substantially less reactive than the primary amine due to steric hindrance. Therefore, the reaction caused by the sec-

Table IV The T_{pi} , Theoretical Char Yield, and Practical Char Yield of Products and LICA 44

Sample Code	LICA 44 in Feed (wt %)	T_{pi} (°C)	Weight Loss of TMPDE (wt %)	Char Yield by LICA 44 ^a (wt %)	Char Yield of Product ^b (wt %)
A	0	353.7	0	—	0
B	17.0	359.7	6.2	5.6	5.1
C	23.5	361.3	8.1	7.3	13.5
D	28.0	362.5	9.7	8.8	14.7
E	38.0	364.3	12.6	11.1	21.8
E05	38.0	355.4	12.6	11.1	11.8
E10	38.0	356.8	12.6	11.1	16.6
E20	38.0	361.5	12.6	11.1	17.8
F	43.4	365.7	14.3	13.0	22.5
G	55.1	367.8	13.5	12.2	35.2
H	64.8	371.6	14.5	13.1	50.8
LICA 44	—	143.0	—	—	34.0

^a The theoretical char yield.

^b The practical char yield.

ondary amine was negligible when the AAR was greater than 1.5. The theoretically product structures under three values of the AAR are described in Figure 1.

The elemental analysis data including estimated compositions of samples are listed in Table II. The element N represents content of LICA 44 in the product. The reaction ratio of LICA 44 was calculated by dividing the measured percent N of the sample over the calculated percent N. The obtained LICA 44 reaction ratio was used to estimate the amount of reacted LICA 44 in SMA-*g*-L44 later in our discussion. Although the percent N in the product increases with AAR in feed, the reaction ratio decreases with the increase of LICA 44 content in feed. This result is reasonable because the steric hindrance during the reaction increases with the increase of LICA 44 grafted in SMA.

The infrared spectrum (a) in Figure 2 is the pure SMA, showing two strong peaks at 1780 and 1860 cm^{-1} that represent the saturated five-member ring anhydride. These two peaks shift to 1700 and 1720 cm^{-1} [spectrum (b) of Fig. 2], a characteristic of the saturated five-member ring imide. However, a continuous jag composed of a series of small bands between 1560 and 1650 cm^{-1} also appear in the products, which is a characteristic of the amide acid. The band 1660 cm^{-1} was taken as a hint for amide acid structure by Vermeesch and Groeninckx when they made a chemical modification of SMA with primary *N*-alkylamines.¹⁸ A band at 700 cm^{-1} , the C—H bending of the phenyl

group of styrene,¹⁹ was chosen as a reference to give the relative strength of the infrared adsorption. The relative peak strength of 1700 cm^{-1} is smaller than that of the original 1780 cm^{-1} . This result indicates that a portion of the reacted maleic anhydride has converted into imide, while the other portion is still in the form of the amide acid. Figure 3 shows the spectra of the products at four different reaction times. The reactivity of anhydride and amine of the system is high, the spectra (b) in Figure 3 (reaction time of 0.5 h) clearly shows imide and amide adsorptions. The relative strength of 1560 and 1650 cm^{-1} amide acid decreases with the increase of reaction time in Figure 3. The result reveals that a longer reaction time leads to the higher yield of imide. The detail values of peak area and relative strengths are listed in Table III.

The Thermal Properties of SMA-*g*-L44

TGA thermograms of samples with different AAR are shown in Figure 4. The initial pyrolysis temperature (T_{pi}) of the samples was determined by the onset-point analysis function of the GENERAL ANALYSIS software, which is shown by curve (a) in Figure 4. The SMA copolymer [curve (a) in Fig. 4], started to decompose at 353.7°C but yielded no char at 800°C under N_2 atmosphere. The T_{pi} and the char yield of curves (b) and (c) are both clearly higher than curve (a). The weight loss observed on curves (b) and (c) before the T_{pi} is the decomposition of LICA 44.

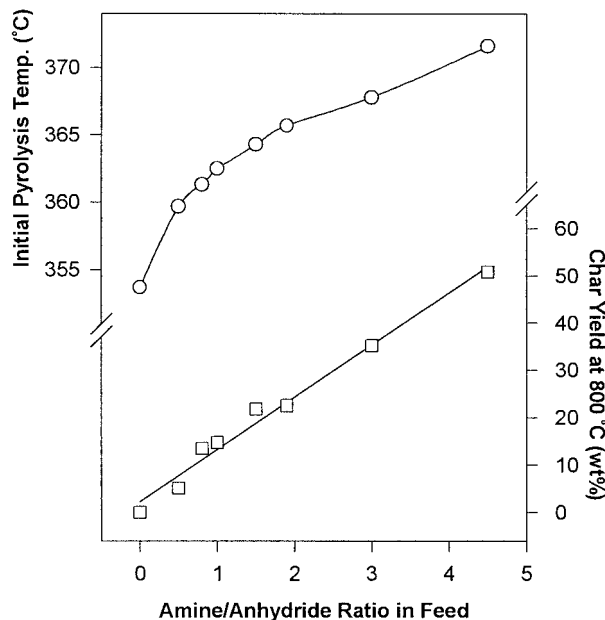


Figure 6 The effects of LICA content of SMA-*g*-L44 on T_{pi} and char yield at 800°C.

Figure 5 shows an inference of the mechanism of the dealcohol reaction of LICA 44. During the heating procedure, the amide acid proceeds with a ring-closing reaction to the imide and releases water. The released water then promotes the decomposition of trimethylolpropane diallyl ether (TMPDE) from LICA 44. The boiling point of TMPDE is known at 135°C, and the theoretical weight loss of TMPDE can be calculated as follow,

$$W_{\text{TMPDE}} = W_L \times \frac{M_{\text{TMPDE}}}{M_L} \times \text{Rxn}\%$$

where W_{TMPDE} and M_{TMPDE} are the theoretical weight loss % and molecular weight of TMPDE; W_L and M_L are the wt % and molecular weight of LICA 44 in feed; $\text{Rxn}\%$ is the reaction percentage of LICA 44 on SMA. The theoretical amount of decomposed TMPDE was calculated and is listed in Table IV.

More detailed variations on T_{pi} and the char yield versus AAR are shown in Figure 6. The main factor influencing T_{pi} is the amount of imide in SMA-*g*-L44 because the imide structure is known for its high thermal resistance. Although the char yield in Figure 6 also increases in a linear tendency versus AAR, the char generation mechanism is very complex. At a temperature of 800°C, about 34% weight of LICA 44 is converted to the

residual as a metallic luster. In contrast, the residual from SMA-*g*-L44 is black. To distinguish the char produced by LICA 44 from that by SMA, the theoretical char yield by LICA 44 is listed in Table IV. For sample B, the char yield of the product is almost the same as that of LICA 44, implying that the char is mainly produced by LICA 44 in this stage. However, the char yield of the product increases rapidly with the increase of the AAR. For example, the char yield of sample H is nearly four times greater than that by LICA 44. In conclusion, the LICA 44 has a promoting effect of char yield on SMA-*g*-L44.

Figure 7 shows that both T_{pi} and the char yield of SMA-*g*-L44 also increase with the increase of the reaction time. The reaction rate of this sample E is quite rapid in the first hour and then goes into a plateau stage. Moreover, Figure 7 also points out that the higher reaction ratio is achievable by extending the reaction time.

The so-called char is a solid residual produced under a high temperature, so two possible char sources of SMA-*g*-L44 can be traced to titanium and the imide group. The titanium in LICA 44 is able to react with oxygen and produces a thermally stable oxide, but the char produced by the titanium is limited and cannot explain the substantial raise in the char yield. For this reason, the imide group is supposed to be the seeds for char production, similar to the effect of the aromatic groups on the main chains of some ther-

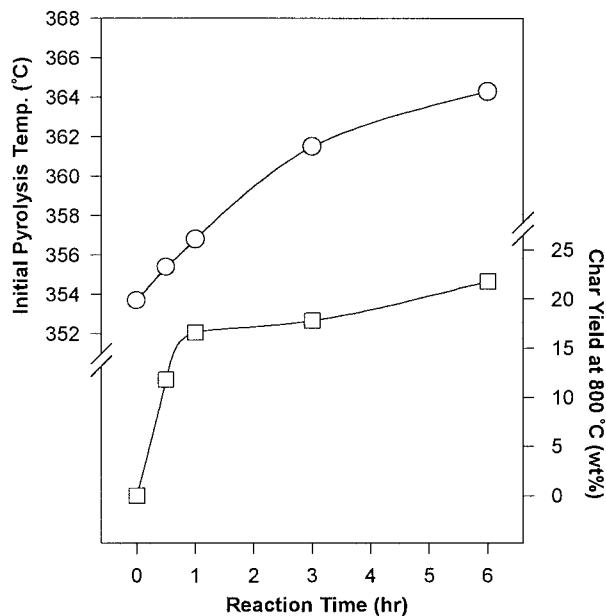


Figure 7 The effects of reaction time of sample E of SMA-*g*-L44 on T_{pi} and char yield at 800°C.

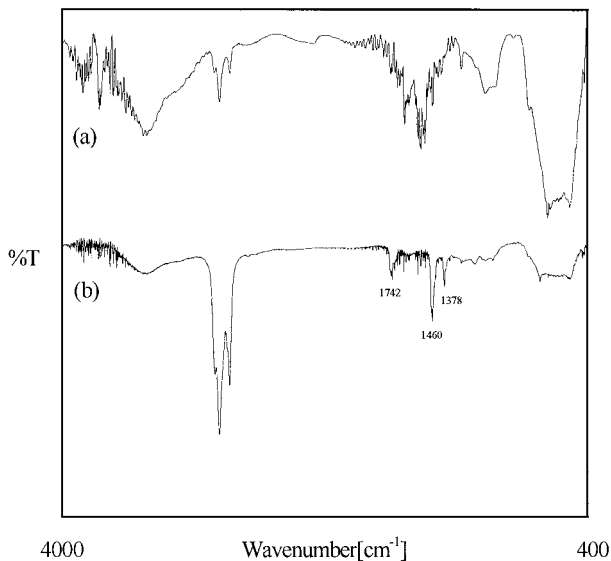


Figure 8 The FTIR spectra of char produced by (a) sample E; and (b) sample H.

mally resistant polymers, and leads to forming a carbon-rich structure. Bridge-building arranged copolymers provide the transfer of protons and electrons, which is usually the important step of char-forming reactions. Even though the infrared spectra in Figure 8 do not provide enough evidence on the final char structure, the bands between $1670\text{--}1430\text{ cm}^{-1}$ ($6\text{--}7\text{ }\mu\text{m}$) indicate the existence of the $\text{C}=\text{C}$ and $\text{C}=\text{N}$ stretching in ring. A reasonable suggestion about the char structure is a multiring of aromatic heterocycles.

CONCLUSION

The results of FTIR and elemental analysis indicated that the reactivity between SMA and LICA 44 is high; however, there is an expelling effect observed under the condition of high AAR. Both combination types of SMA-*g*-L44, amide acid, and imide, can be clearly found in infrared spectra. We cannot determine the exact ratio of these two types, but can only observe the variation by comparing the relative strength of the bands of 1560, 1650, and 1700 cm^{-1} . A weight loss of SMA-*g*-L44 in TGA starting at about 130°C was found to be the decomposition of trimethylolpropane diallyl ether (TMPDE). The initial pyrolysis temperature (T_{pi}) and char yield of SMA-*g*-L44 increased

with the raise of AAR in feed and reaction time. The increase of T_{pi} is mainly due to the formation of the imide group in SMA-*g*-L44. The char yield promoting effect of LICA 44 is attributed to the titanium, the imide group, and bridge-building in SMA-*g*-L44. The maximum char yield of SMA-*g*-L44 reached 50.8 wt %. Although only 13.1 wt % was produced by titanium, another 37.7 wt % was promoted by the graft reaction of LICA 44 on SMA.

The authors wish to express their appreciation to Dr. T. S. Lin, President of Tatung Institute of Technology, for his encouragement and support. Thanks are also due to the National Science Council for financial support under contract number NSC86-2216-E-036-001.

REFERENCES

1. Q. Lin, M. Talukder, and C. U. Pittman, *J. Polym. Sci., Part A: Polym. Chem.*, **33**, 2375 (1995).
2. S. Yukioka and T. Inoue, *Polymer*, **35**, 1182 (1994).
3. J. M. Machado and C. S. Lee, *Polym. Eng. Sci.*, **34**, 59 (1994).
4. B. Majumdar, H. Keskkula, and D. R. Paul, *Polymer*, **35**, 3164 (1994).
5. L. Nie and R. Narayan, *Polymer*, **35**, 4334 (1994).
6. L. Nie and R. Narayan, *J. Appl. Polym. Sci.*, **54**, 601 (1994).
7. C. Koning, A. Ikker, R. Borggreve, L. Leemans, and M. Möller, *Polymer*, **34**, 4410 (1993).
8. Y. Lee and K. Char, *Macromolecules*, **27**, 2603 (1994).
9. W. Y. Chiang and G. L. Tzeng, *J. Appl. Polym. Sci.*, to appear.
10. W. Y. Chiang and C. H. Hu, *Eur. Polym. J.*, **32**, 385 (1996).
11. W. Y. Chiang and W. D. Yang, *J. Appl. Polym. Sci.*, **35**, 807 (1988).
12. W. Y. Chiang, W. D. Yang and B. Pukanszky, *Polym. Eng. Sci.*, **32**, 641 (1992).
13. W. Y. Chiang, W. D. Yang and B. Pukanszky, *Polym. Eng. Sci.*, **34**, 485 (1994).
14. W. Y. Chiang and Y. S. Chiang, *J. Appl. Polym. Sci.*, **46**, 673 (1992).
15. K. Ghosh and N. Maiti, *J. Appl. Polym. Sci.*, **60**, 323 (1996).
16. W. Y. Chiang and J. Y. Ao, *J. Polym. Res.*, **2**, 83 (1995).
17. W. Y. Chiang and C. Y. Hsiao, *Angew. Makromol. Chem.*, **219**, 169 (1994).
18. I. Vermeesch and G. Groeninckx, *J. Appl. Polym. Sci.*, **53**, 1365 (1994).
19. H. Feng, L. Shen, and Z. Feng, *J. Appl. Polym. Sci.*, **31**, 243 (1995).